

# Tail-Aware Density Forecasting of Locally Explosive Time Series: A Neural Network Approach

Elena Dumitrescu\*

University Paris-Panthéon-Assas, CRED, 75005 Paris, France

and

Julien Peignon

CEREMADE, CNRS, UMR 7534, Université Paris-Dauphine  
PSL University, Paris, France

and

Arthur Thomas

Université Paris-Dauphine, Université PSL  
LEDa, CNRS, IRD, 75016 Paris, France

January 21, 2026

## Abstract

This paper proposes a Mixture Density Network for forecasting time series that exhibit locally explosive behavior. By incorporating skewed t-distributions as mixture components, our approach offers enhanced flexibility in capturing the skewed, heavy-tailed, and potentially multimodal nature of predictive densities associated with bubble dynamics modeled by mixed causal-noncausal ARMA processes. In addition, we implement an adaptive weighting scheme that emphasizes tail observations during training and hence leads to accurate density estimation in the extreme regions most relevant for financial applications. Equally important, once trained, the MDN produces near-instantaneous density forecasts. Through extensive Monte Carlo simulations and an empirical application on the natural gas price, we show that the proposed MDN-based framework delivers superior forecasting performance relative to existing approaches.

*Keywords:* Forecasting, Noncausal Models, Mixture Density Networks

---

\*We are grateful to Serge Darolles, Christian Francq, Gaëlle le Fol, Daniel Velasquez Gaviria, Christian Gouriéroux, Alain Hecq, Joann Jasiak, Sébastien Laurent, Yannick Le Pen, Gabriele Mingoli, Aryan Manafi Neyazi, Fabrice Rossi and Jean-Michel Zakoian. We also thank the seminar participants at Dauphine University - PSL and Maastricht University School of Business and Economics, as well as the participants at the 19th International Conference on Computational and Financial Econometrics, and the First Workshop in Noncausal Econometrics for helpful comments and discussions.

# 1 Introduction

Time-series forecasts using causal ARMA models have been playing a crucial role in economic and financial decision-making processes for a long time. There is a very rich literature on various aspects of forecasting and forecast evaluation that tackle such real-life challenges (for an overview of this literature, see e.g. Petropoulos et al. 2022, Castle et al. 2019, Diebold 2017). A conclusion often reached in this context where the current value of the variable of interest is forced to depend only on its past is that one- and multi-step ahead forecasting in periods of high instability is particularly difficult. Indeed, these causal models are characterized by mean reversion, and their forecasts converge to the unconditional mean even after an extreme event occurs, regardless of whether such behavior reflects the true underlying dynamics. In the specific case of financial market data, which we are interested in, the traditional properties of heavy-tailed marginal distributions and volatility clustering are at the core of forecasting models. But a close look at the dynamics of various types of asset prices, sometimes called speculative assets, reveals the presence of phases of locally explosive behaviour, *i.e.*, rising patterns followed by a burst, local trends and spikes. Such non-linear characteristics are, however, very poorly captured by standard financial econometric models (the ARMA-GARCH family).

Recently, (causal-)noncausal autoregressive processes have been found to be suitable for modelling such locally explosive behaviour as they allow for dependence on the future. These simple linear models produce rich non-linear patterns without requiring non-linearities to be imposed *ex ante*. Importantly, noncausal processes are grounded in macroeconomic theory, as they arise as stationary solutions of rational expectation models under infinite variance Gourieroux et al. (2020). Relevant applications of these models range from asset prices (see Fries & Zakoian 2019, Gourieroux & Zakoian 2017, Gourieroux & Jasiak 2018, Hecq & Velasquez-Gaviria 2025), to macroeconomic data (see Lanne & Saikkonen 2011,

Lanne & Luoto 2016, Davis & Song 2020), commodity prices (Blasques et al. 2025), climate risk on El Niño and La Niña (de Truchis et al. 2025), green stock prices (Giancaterini et al. 2025), and to electronic currency exchange rates (Cavaliere et al. 2020).

However, although being able to compute forecasts is crucial for empirical economics, building predictions with this class of models has been shown to be particularly difficult due to their dependence on future values. In fact, it has long been thought that the conditional predictive density of mixed causal-noncausal processes does not have closed-form and inference can only be performed by simulation-based or Bayesian methods (see Lanne et al. 2012, Gourieroux & Jasiak 2016, Nyberg & Saikkonen 2014). Although these approaches constitute flexible alternatives for predicting general noncausal processes, Hecq & Voisin (2021) highlight two main drawbacks. They become computationally intensive for large prediction horizons, and they fail to accurately capture the dynamics during explosive episodes, *i.e.*, that of the tails of the distribution. This limitation is highly problematic given that modeling explosive tail behavior is the primary motivation for using noncausal processes in the first place.

More importantly, noncausal processes exhibit highly non-linear and process-specific tail behavior that must be properly accounted for in forecasting. For example, when the conditional predictive density becomes multimodal, point forecasts become meaningless, as they fail to represent the fundamental dichotomy between bubble continuation and collapse (see Gourieroux & Zakoian 2017, Fries 2022, de Truchis et al. 2025, Gourieroux et al. 2025). For this reason, the noncausal literature as a whole, and this paper in particular, focuses exclusively on density forecasting rather than point prediction. Additionally, these tail behaviors may also explain the difficulties encountered by standard numerical approaches when modelling extreme values (see Hecq & Voisin 2021) and provides insight into why

state-of-the-art machine learning methods do not adequately forecast locally explosive dynamics (Saïdi 2023).

This paper takes a new approach to forecasting noncausal processes. Rather than relying on computationally intensive simulation-based methods or closed-form approximations with restrictive assumptions, we exploit recent advances in statistical learning to accurately estimate the full conditional predictive density of univariate general mixed causal-noncausal autoregressive moving average (MARMA) processes. More precisely, we introduce a newly tailored Mixture Density Network (MDN) based on skewed t-distributions as mixture components, which naturally captures both the multimodality and heavy-tailed asymmetric nature of predictive densities during explosive episodes. Note that, in contrast, traditional Mixture Density Networks (à la Bishop 1994) involve exponentially decaying tails of Gaussian mixtures. They hence struggle to adequately capture the heavy-tailed behavior prevalent in financial series, and lead to systematic underestimation of extreme event probabilities. At the same time, traditional MDNs do not account for the natural imbalance between normal market conditions and extreme events that characterize financial time series and have deep implications for risk assessment. For these reasons, their use in finance has been very limited. To address this challenge, we develop an adaptive weighting scheme that gives more weight to tail observations during training, and hence enables accurate density estimation in the extreme regions most relevant for financial application. Another significant advantage of our approach is that, once trained, the MDN produces near-instantaneous density forecasts for all forecasting horizons under analysis. In contrast, existing simulation-based approaches are much more time-consuming.

Through extensive Monte Carlo simulations and an empirical application on the natural gas price, we show that the proposed MDN-based framework delivers superior forecasting performance relative to existing approaches: i. the traditional Nadaraya-Watson kernel

density estimator (Rosenblatt 1969), ii. the simulation-based approach of Lanne et al. (2012), iii. the closed-form (and SIR-based) approach of Gourieroux & Jasiak (2025) and iv. the nonparametric conditional density estimation approach of Dalmasso et al. (2020).

Furthermore, our density forecasts are shown to provide a very good approximation to the true conditional predictive moments, especially in the tails of the distribution.

Our contribution to the literature is threefold. We propose a novel neural network approach with tailored weighting and sampling schemes designed to capture the locally explosive dynamics of noncausal time series. This paper is actually the first to propose a learning method for the conditional predictive density of MARMA processes, as existing approaches only address mixed causal-noncausal AR processes. Second, we show that the MDN-based method exhibits superior forecasting performance relatively to standard methods available in the literature while requiring substantially less computational time. We also find that it approximates the true predictive density more reliably than the other approaches. Third, as a byproduct, we extend Lanne et al. (2012)'s forecasting procedure to  $\alpha$ -stable laws (see the Online Appendix).

The paper is structured as follows. Section 2 details our machine learning forecasting method. The Monte Carlo analysis is detailed in Section 3. Section 4 summarizes the empirical illustration, while Section 5 concludes and discusses avenues for future research.

## 2 Forecasting with Mixture Density Networks

Traditional Mixture Density Networks (Bishop 1994) provide a flexible framework for modeling conditional probability distributions by outputting the parameters of a Gaussian mixture model through a neural network. However, Gaussian mixtures struggle to adequately capture the heavy-tailed behavior of financial series and lead to systematic underestimation

of extreme event probabilities. To address this deficiency, we propose a new MDN, which relies on skewed t-distribution components instead of Gaussian ones to provide flexible parametric control over both skewness and tail heaviness. More precisely, it models the conditional density as:

$$p(X_{t+h}|\mathbf{X}_t) = \sum_{j=1}^K \pi_j(\mathbf{X}_t) \cdot f(X_{t+h}; \mu_j(\mathbf{X}_t), \sigma_j(\mathbf{X}_t), \xi_j(\mathbf{X}_t), \nu_j(\mathbf{X}_t)), \quad (1)$$

with  $f(y; \mu, \sigma, \xi, \nu) = \frac{2}{\sigma} t\left(\frac{y-\mu}{\sigma}; \nu\right) T\left(\xi \frac{y-\mu}{\sigma} \sqrt{\frac{\nu+1}{\nu+\frac{y-\mu}{\sigma}}}; \nu+1\right)$  the skewed t-distribution probability density function, where  $t(\cdot; \nu)$  denotes the Student-t density and  $T(\cdot; \nu)$  its cumulative distribution function, both with  $\nu$  degrees of freedom that control tail thickness. The other parameters are the location  $\mu \in \mathbb{R}$ , the scale  $\sigma > 0$ , and the shape  $\xi \in \mathbb{R}$ , which governs asymmetry.<sup>1</sup>

We develop our own network architecture and training strategy tailored to the time series forecasting context as follows.

## 2.1 Network Architecture

Our network architecture is lightweight and parsimonious, consisting of two hidden layers of dimension 64, making it efficient to train even on standard CPU hardware (see Figure 1). It has two main components. The first one includes the two hidden layers, each with rectified linear unit (ReLU) activations:  $\mathbf{h}^{(\ell+1)} = \text{ReLU}(\mathbf{W}^{(\ell)} \mathbf{h}^{(\ell)} + \mathbf{b}^{(\ell)})$ , with  $\mathbf{h}^{(0)} = \mathbf{X}_t$ . The second one consists of five parallel output heads that map the final hidden representation

---

<sup>1</sup>We found this parameterization of the MDN to be numerically more robust than the Tukey g-and-h component-based approach of [Guillaumin & Efremova \(2024\)](#), as it does not need computing numerical inverse transforms via binary search, which can cause training instability when dealing with extreme values in the tails. Additionally, the skewed t-distribution distribution admits well-established multivariate extensions (see [Azzalini & Dalla Valle 1996](#)), providing a natural pathway for extending our framework to vector-valued time series in future work.

$\mathbf{h}^{(\ell_{\text{last}})}$  to the mixture parameters:

$$\boldsymbol{\pi}(\mathbf{X}_t) = \text{Softmax}(\mathbf{W}_\pi \mathbf{h}^{(\ell_{\text{last}})} + \mathbf{b}_\pi) \in [0, 1]^K, \sum_{i=1}^K \pi_i = 1 \quad (2)$$

$$\boldsymbol{\mu}(\mathbf{X}_t) = \mathbf{W}_\mu \mathbf{h}^{(\ell_{\text{last}})} + \mathbf{b}_\mu \in \mathbb{R}^K \quad (3)$$

$$\boldsymbol{\sigma}(\mathbf{X}_t) = \text{Softplus}(\mathbf{W}_\sigma \mathbf{h}^{(\ell_{\text{last}})} + \mathbf{b}_\sigma) \in \mathbb{R}_+^K \quad (4)$$

$$\boldsymbol{\xi}(\mathbf{X}_t) = \mathbf{W}_\xi \mathbf{h}^{(\ell_{\text{last}})} + \mathbf{b}_\xi \in \mathbb{R}^K \quad (5)$$

$$\boldsymbol{\nu}(\mathbf{X}_t) = \text{Softplus}(\mathbf{W}_\nu \mathbf{h}^{(\ell_{\text{last}})} + \mathbf{b}_\nu) \in \mathbb{R}_+^K, \quad (6)$$

where  $K = 10$  is the number of mixture components. The activation functions are chosen to enforce appropriate parameter constraints: softmax ensures valid mixture weights, softplus guarantees positive scale and degree of freedom parameters, while the location and skewness parameters are left unconstrained.

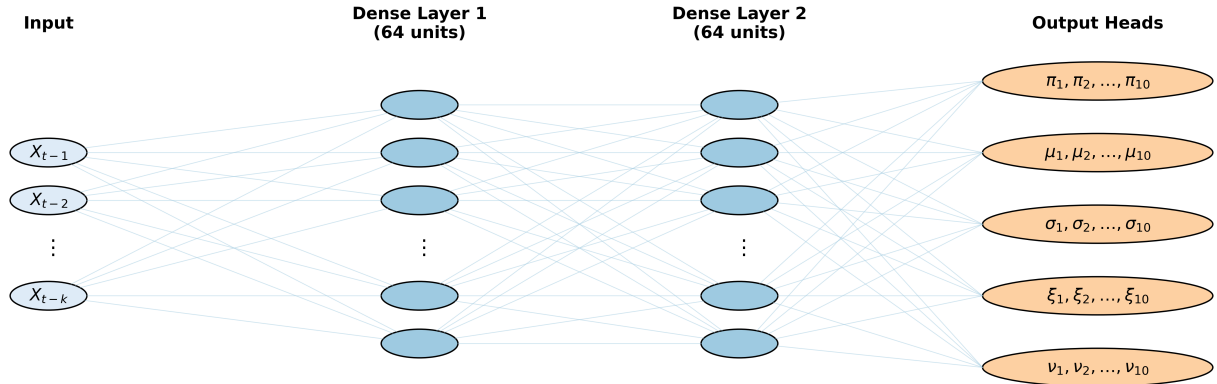


Figure 1: Our Mixture Density Network architecture

Finally, we regularize the MDN through noise regularization, which adds Gaussian perturbations to the training data. This approach smooths the estimated density by penalizing the Hessian of the log-likelihood and has been promoted in the conditional density estimation framework (Rothfuss et al. 2019, 2020). The complete set of MDN hyperparameters is detailed in Table 1 below.

Table 1: Hyperparameters of the Mixture Density Network

Category	Hyperparameter (Value)
Architecture	Hidden Layers: [64, 64]
	Number of Mixtures: 10
Training	Optimizer: Adam
	Learning Rate: $10^{-3}$
	Epochs: 50

## 2.2 Adaptive Weighting Function

Financial time series contain a natural imbalance between normal market conditions and extreme events. At the same time, standard learning algorithms tend to prioritize frequent observations at the expense of rare ones, although the latter are of greater importance for risk assessment (Branco et al. 2019, Ribeiro & Moniz 2020). To address this, we adapt the inverse proportion weighting scheme, well-established in cost-sensitive learning of imbalanced data (Steininger et al. 2021).

Let  $\mathcal{D}$  denote the training sample, and let the subset of tail events in the training sample be given by  $\mathcal{T} = \{t \in \mathcal{D} : X_t < \ell \text{ or } X_t > u\}$ . The boundaries  $\ell$  and  $u$  are determined using the generalized boxplot methodology of Bruffaerts et al. (2014).<sup>2</sup> Then, the adaptive weight function is given by:

$$w_t = \begin{cases} \sqrt{\frac{|\mathcal{D}|}{|\mathcal{T}|}}, & \text{if } t \in \mathcal{T} \\ 1, & \text{otherwise.} \end{cases} \quad (7)$$

The weighting mechanism operates at two levels during training, which allows the model to focus on rare tail events without requiring modifications to the underlying MDN architecture (Branco et al. 2019, Moniz et al. 2017). First, during mini-batch construction, we give more weight to rare cases by employing a weighted random sampling with replacement approach (Avelino et al. 2024, Branco et al. 2019). Under this scheme, the probability that

<sup>2</sup> $\ell = \xi_{\delta/2}^{\text{TGH}}$ ,  $u = \xi_{1-\delta/2}^{\text{TGH}}$ , for a fixed detection rate  $\delta$ , where  $\xi^{\text{TGH}}$  is the empirical Tukey g-h CDF fitted to a rank-preserving transformation of the observed data to accurately capture skewness and tail heaviness of the data.

observation  $t$  is sampled in a mini-batch  $\mathcal{B}$  is given by  $P(t) = w_t / \sum_{i=1}^{|\mathcal{D}|} w_i$ . Second, within each mini-batch  $\mathcal{B}$ , we apply cost-sensitive learning through a weighted loss function (Shi et al. 2024, Steininger et al. 2021). The model parameters,  $\theta$ , are updated by minimizing the weighted negative log-likelihood:

$$\mathcal{L}(\theta) = -\frac{1}{\sum_{t \in \mathcal{B}} w_t} \sum_{t \in \mathcal{B}} w_t \log p(X_{t+h} | \mathbf{X}_t; \theta), \quad (8)$$

where  $t$  indexes the observations in the mini-batch. This dual application of weights – both in sampling and loss computation – results in an effective weight of  $|\mathcal{D}|/|\mathcal{T}|$  for tail events, justifying the square-root scaling in (7) to achieve the desired inverse proportion weighting.

### 2.3 Post-hoc Calibration via Local PIT Modeling

By reweighting the training distribution to emphasize extreme events, we train the model on a distribution that differs from the true data-generating process. Specifically, when we assign higher weights to tail observations, the model learns to predict conditional distributions  $\hat{p}(X_{t+h} | \mathbf{X}_t)$  that reflect this reweighted empirical distribution rather than the original empirical distribution. This shift causes systematic biases: the model overestimates the probability of extreme events across the entire input space, leading to miscalibrated predictions when evaluated with respect to the original, unweighted distribution.

To correct for miscalibration, we use the method of Dey et al. (2022, 2025) based on the uniformity property of the Probability Integral Transform (PIT),  $\text{PIT}(X_{t+h}, \mathbf{X}_t) = \int_0^{X_{t+h}} \hat{p}(z | \mathbf{X}_t) dz = \hat{F}(X_{t+h} | \mathbf{X}_t)$ , where  $\hat{F}$  is the predicted cumulative distribution function.<sup>3</sup>

---

<sup>3</sup>Under perfect calibration, the PIT follows a uniform distribution,  $\text{PIT} \sim \mathcal{U}([0, 1])$ , deviations from uniformity indicating miscalibration. This calibration-accuracy trade-off is well-documented in the machine learning literature (Guo et al. 2017, Kull et al. 2019): improving performance on specific regions of the distribution often degrades overall calibration. Post-hoc calibration methods are therefore essential to restore the reliability of probabilistic predictions while preserving the improved tail modeling capabilities achieved through weighted training.

This recalibration procedure is applied after the initial model training on  $\mathcal{D}$  and requires a distinct dataset,  $\mathcal{D}_{\text{cal}}$ . First, we use the trained model to compute the PIT values for all observations in  $\mathcal{D}_{\text{cal}}$ . Then, the empirical PIT distribution is estimated through an ensemble of XGBoost classifiers (Chen & Guestrin 2016) conditionally on the input features:

$$\hat{\beta}(\tau|\mathbf{X}'_t) = \mathbb{P}(\text{PIT} \leq \tau|\mathbf{X}'_t) = \mathbb{P}(\hat{F}(X'_{t+h}|\mathbf{X}'_t) \leq \tau|\mathbf{X}'_t), \quad \tau \in [0, 1], \quad (9)$$

for observations  $(X'_{t+h}, \mathbf{X}'_t) \in \mathcal{D}_{\text{cal}}$ . Perfect calibration corresponds to  $\hat{\beta}(\tau|\mathbf{X}'_t) = \tau$ . To ensure monotonicity and smoothness, the estimated PIT distribution is represented using I-spline basis functions (Ramsay 1988) with non-negative weights obtained through constrained regression.

Once the correction function  $\hat{\beta}$  is learned on  $\mathcal{D}_{\text{cal}}$ , it can be applied to any new observation with features  $\mathbf{X}_t$  (from the test set or future data). The final recalibrated PDF is obtained by applying the correction and then renormalizing,

$$\hat{p}_{\text{recal}}(X_{t+h}|\mathbf{X}_t) = \frac{c(X_{t+h}|\mathbf{X}_t) \cdot \hat{p}(X_{t+h}|\mathbf{X}_t)}{\int c(z|\mathbf{X}_t) \cdot \hat{p}(z|\mathbf{X}_t) dz}, \quad (10)$$

with correction factor

$$c(X_{t+h}|\mathbf{X}_t) = \left. \frac{d\hat{\beta}}{d\tau} \right|_{\tau=\hat{F}(X_{t+h}|\mathbf{X}_t)}. \quad (11)$$

This local approach allows for feature-dependent calibration adjustments, thus accommodating heterogeneous miscalibration patterns while preserving the enhanced tail modeling capabilities achieved through weighted training.

### 3 Monte Carlo Simulations

In this section, we investigate the forecasting abilities of our MDN approach in various setups where the theoretical density of MARMA models is known or at least the theoretical conditional moments can be calculated by following [Fries \(2022\)](#). To study the relative performance of our method, we proceed with a horse race with existing forecasting approaches.

#### 3.1 MARMA Processes

The complex non-linear distributional characteristics of financial time series, *i.e.*, multimodality, skewness, and heavy tails, corresponding often to extreme market events, can be modelled by Mixed Causal-Noncausal Autoregressive Moving Average processes. Let  $X_t$  ( $t = 0, \pm 1, \pm 2, \dots$ ) be a stochastic process generated by

$$\psi(F)\phi(B)X_t = \theta(F)H(B)\varepsilon_t, \quad (12)$$

where  $F$  (resp.  $B = F^{-1}$ ) denotes the forward (resp. backward) operator,  $\psi(z) = 1 - \psi_1 z - \dots - \psi_p z^p$ ,  $\phi(z) = 1 - \phi_1 z - \dots - \phi_q z^q$ ,  $\theta(z) = 1 - \theta_1 z - \dots - \theta_r z^r$ , and  $H(z) = 1 - H_1 z - \dots - H_s z^s$  are polynomials with roots outside the unit circle, and  $(\varepsilon_t)_{t \in \mathbb{Z}}$  is a sequence of i.i.d. variables. Equation (12) admits a unique stationary solution, called a *MARMA*( $p, q, r, s$ ), if  $\phi(z) \neq 0$  and  $\psi(z) \neq 0$  for all  $|z| \leq 1$ , and if  $\psi$  (resp.  $\phi$ ) has no common root with  $\theta$  (resp.  $H$ ). A sufficient condition for the identification of the model in (12) is that  $\varepsilon_t$  is i.i.d. non-gaussian (see [Rosenblatt 2000](#)). The literature has been using either  $\alpha$ -stable or  $t$ -distributed innovations, the choice of one or another driving the forecasting algorithms proposed so far in the literature.

Since for  $t$ -distributed errors there are very few theoretical results available in the literature on predictive densities, we choose to follow the literature on  $\alpha$ -stable MARMA models. This offers us a unique forecast evaluation framework in which a closed-form expression for the conditional predictive density exists, i.e. when  $\varepsilon_t \sim$  Cauchy distribution (Gourieroux & Zakoian 2017). More generally, as de Truchis et al. (2025) show, when  $\varepsilon_t \stackrel{i.i.d.}{\sim} \mathcal{S}(\alpha, \beta, \sigma, \mu)$ ,  $\alpha > 1$ ,  $\beta \in [-1, 1]$ ,  $\sigma > 0$  one may rely on the theoretical results of Fries (2022) and derive closed-form formulas for higher-order conditional moments of two-sided MA( $\infty$ )  $\alpha$ -stable processes such as that in (12),  $\mathbb{E}[X_{t+h}^p | X_t = x]$ , with  $p$  an integer that satisfies  $1 \leq p < 2\alpha + 1$ ,  $h$  the forecast horizon, and where the joint predictive density of  $(X_{t+h}, X_t)'$  has been shown to be a multivariate  $\alpha$ -stable process.<sup>4</sup> This constitutes a very nice framework for the evaluation of density forecasts obtained from very different forecasting algorithms which are not directly comparable through traditional approaches.

### 3.2 Simulation Design

We generate time series of length 5,000 from the following MARMA data generating processes (de Truchis & Thomas 2025):

$$\text{MAR}(0,1): \quad (1 - 0.9F)X_t = \varepsilon_t, \quad (13)$$

$$\text{MAR}(0,2): \quad (1 - 0.9F - 0.7F^2)X_t = \varepsilon_t, \quad (14)$$

$$\text{MAR}(1,1): \quad (1 - 0.9F)(1 - 0.1B)X_t = \varepsilon_t, \quad (15)$$

$$\text{MARMA}(1,1,1,1): \quad (1 - 0.9F)(1 + 0.3B)X_t = (1 - 0.4F)(1 + 0.3B)\varepsilon_t, \quad (16)$$

where  $\varepsilon_t \stackrel{i.i.d.}{\sim} \mathcal{S}(\alpha, 0, 0.5, 0)$ .<sup>5</sup> Although the choice of the distribution does not affect the predictive methods themselves, the  $\alpha$ -stable family offers greater flexibility, as it encompasses

---

<sup>4</sup>see Fries (2022), Samorodnitsky & Taqqu (1996).

<sup>5</sup>The parameter values are chosen by following de Truchis et al. (2025) for the three MAR models and based on Fries (2022) for the MARMA specification. All specifications satisfy the stationarity conditions.

a variety of shapes including the Gaussian ( $\alpha = 2, \beta = 0$ ) and Cauchy ( $\alpha = 1, \beta = 0$ ) distributions as special cases. In the simulations, we set  $\alpha \in \{1.0, 1.2, 1.4, 1.8\}$ , where smaller values correspond to fatter tails, which allows us to examine how model performance changes with the degree of tail heaviness.

The forecasting abilities of our MDN approach are compared with those of a set of established conditional density forecasting methods spanning different methodological paradigms: the nonparametric Nadaraya-Watson kernel density estimator (Nadaraya 1964, Watson 1964), the simulation-based approach of Lanne et al. (2012) and the closed-form predictive densities of Gourieroux & Jasiak (2025), both designed for MAR processes, as well as the learning-based FlexZBoost method of Izbicki (2017) and Dalmasso et al. (2020).<sup>6</sup> An additional calibration set  $\mathcal{D}_{\text{cal}}$  of 5,000 observations, generated by the same data-generating process, is used to perform the local recalibration procedure described in Section 2.3 for the MDN.

To ensure a fair comparison across all methods, the kernel densities required by Nadaraya-Watson and the noncausal state density needed for the closed-form approach of Gourieroux & Jasiak (2025) are both estimated using the same 5,000-observation training set. The simulation-based method of Lanne et al. (2012) does not require additional historical observations beyond the parameter estimation step and can be applied directly to the evaluation grid once the MAR and  $\alpha$ -stable parameters are obtained. Note that for Lanne et al. (2012) and Gourieroux & Jasiak (2025), the MAR specification is assumed known, thereby circumventing model identification issues. We estimate the MAR process parameters using the Generalized Covariance (GCov) estimator (Gourieroux & Jasiak 2023, Manafi Neyazi 2025), a semi-parametric approach that minimizes a portmanteau statistic based on the autocovariances of transformed residuals. The parameters of the  $\alpha$ -stable distribution are then obtained by fitting the characteristic function-based estimator of Nolan

---

<sup>6</sup>For a thorough presentation of these methods, see the Online Appendix.

(2020) to the filtered residuals.<sup>7</sup> In contrast, the nonparametric and learning-based methods, Nadaraya-Watson, FlexZBoost, and our MDN, do not require explicit parametric model estimation and directly learn the predictive density from the data.<sup>8</sup>

### 3.3 Bimodality Analysis

As mentioned in the introduction, for any MAR process with a single anticipative root, when conditioning on a single observation, the conditional predictive density theoretically exhibits bimodality in the tail regions, which reflects the fundamental dichotomy of locally explosive dynamics: the bubble either continues with probability  $|\psi_1|^{\alpha h}$  or crashes (See Section 2.2 in the Online Appendix for a discussion on this point.)

Before implementing the forecast evaluation horse-race, we investigate whether the competing approaches capture well this theoretical bimodality of the conditional predictive density, particularly in the tail region. The procedure relies on a grid of 5,000 equispaced conditioning values  $\{x_1, \dots, x_{5000}\}$  spanning the quantile range  $[q_{0.01}, q_{0.99}]$ . For each point  $x_i$  on the grid, we estimate the conditional predictive density  $\hat{p}(X_{t+1} | X_t = x_i)$  using each of the competing methods and visually assess their ability to recover the bimodal structure across three distinct regions: the center  $[q_{0.10}, q_{0.90}]$ , the tails  $[q_{0.01}, q_{0.10}] \cup [q_{0.90}, q_{0.99}]$ , and the total range  $[q_{0.01}, q_{0.99}]$ .

Figure 2 displays the one-step-ahead conditional predictive density for a MAR(0,1) process under three conditioning scenarios:  $X_t = q_{0.01}$  (left tail),  $X_t = 0$  (center), and  $X_t = q_{0.99}$  (right tail), where  $q_\tau$  denotes the  $\tau$ -quantile of the theoretical marginal distribution.

---

<sup>7</sup>This is an optimal framework to account for parameter estimation uncertainty, whereas in real-life applications model risk also matters and can further hamper the forecasting abilities of these approaches.

<sup>8</sup>To assess the impact of parameter estimation uncertainty, we conducted additional simulations where the methods of Lanne et al. (2012) and Gourieroux & Jasiak (2025) were evaluated using the true data-generating parameters rather than estimated ones. The relative performance rankings remained unchanged, indicating that the observed differences in forecasting accuracy are not primarily attributable to parameter estimation error.

The MDN (panel a) successfully captures this bimodality,<sup>9</sup> exactly as predicted by the

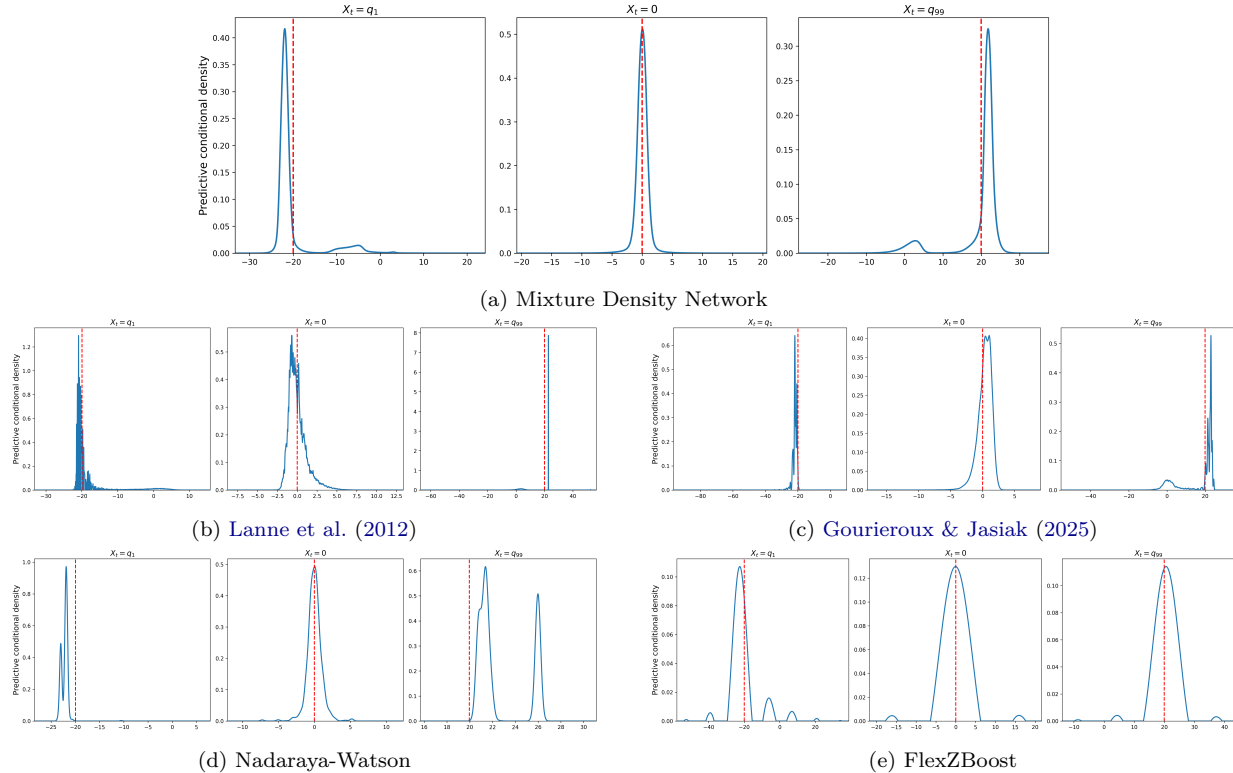


Figure 2: 1-Step-Ahead Conditional Predictive Density of a MAR(0,1) Process

*Notes:* This figure displays the estimated conditional predictive density  $\hat{p}(X_{t+h}|X_t)$  for a purely noncausal MAR(0,1) process with  $\alpha$ -stable innovations at three conditioning values:  $X_t = q_1$  (left tail),  $X_t = 0$  (center), and  $X_t = q_{99}$  (right tail), where  $q$  denotes the percentiles. The red dashed line indicates the conditioning value  $X_t$ . The tail-index is fixed at  $\alpha = 1.4$ .

geometric decay of  $|\psi_1|^{\alpha h}$ . Moreover, employing skewed t-distribution mixture components proves beneficial: the MDN naturally outputs asymmetric and heavy-tailed predictive densities. In contrast, Nadaraya-Watson (panel d) produces a highly erratic predictive density, with substantial gaps and spikes, especially in data-sparse tail regions. The approaches of Lanne et al. (2012) and Gourieroux & Jasiak (2025) exhibit similar irregular behavior. FlexZBoost (panel e) yields smoother estimates than kernel methods but displays small spurious bumps due to its inability to set certain cosine basis coefficients to zero. This prevents it from achieving the clean bimodal structure predicted by theory and confirms that general-purpose density estimators require substantial adaptation to capture locally explosive patterns.

<sup>9</sup>The bimodality becomes increasingly pronounced as the horizon extends from  $h = 1$  to  $h = 5$ , and it is best captured by the MDN approach (see Section 3 in the Online Appendix).

### 3.4 Simulation Results

Ideally, comparing the alternative forecasting approaches introduced in Section 3.2 would involve evaluating the competing predictive densities against the true theoretical one. However, since the latter is unavailable for most noncausal processes, our simulation analysis proceeds along three complementary directions.

First, we exploit a unique feature of the Cauchy MAR(0,1) process ( $\alpha = 1.0$ ,  $\beta = 0$ ): the availability of a closed-form expression for the conditional predictive density (Gourieroux & Zakoian 2017). This special case provides a direct benchmark for assessing how well each method approximates the true density. Second, for the general case of MARMA processes where closed-form densities are unavailable, we rely on theoretical conditional moments to evaluate predictive accuracy. Specifically, we compute the estimated conditional moments by numerically integrating the estimated predictive densities, and compare them to their theoretical counterparts. Third, we complement the grid-based evaluation with an out-of-sample forecasting exercise that assesses the predictive densities against realized outcomes, thereby mimicking more closely real-world forecasting scenarios.

#### 3.4.1 Case 1: Cauchy MAR(0,1) model

Table 2 compares the estimated predictive densities with the true density of a MAR(0,1) process with  $\alpha = 1.0$  and  $\beta = 0$ , using Kullback-Leibler (KL) divergence and Integrated Squared Error (ISE) metrics.<sup>10</sup>

Using the grid-based methodology described above, we estimate the conditional predictive density  $\hat{p}(X_{t+1} | X_t = x_i)$  for each competing method and directly compare it with the true

---

<sup>10</sup>The KL divergence is defined as  $\text{KL}(p\| \hat{p}) = \int p(x_{t+h}|x_t) \log \left( \frac{p(x_{t+h}|x_t)}{\hat{p}(x_{t+h}|x_t)} \right) dx_{t+h}$ , while the ISE is given by  $\text{ISE} = \int (p(x_{t+h}|x_t) - \hat{p}(x_{t+h}|x_t))^2 dx_{t+h}$ .

Table 2: KL Divergence and ISE Between the True Predictive Density and the Predicted Ones:  
the Case of MAR(0, 1)

Horizon	Model	KL Divergence			ISE		
		Center	Tails	Total	Center	Tails	Total
$h = 1$	Nadaraya-Watson	<b>0.578</b>	11.45	10.39	<b>0.020</b>	0.751	0.680
	Lanne et al. (2012)	2.339	13.10	12.06	0.418	0.416	0.416
	Gourieroux and Jasiak (2025)	2.512	8.392	7.823	0.441	0.600	0.585
	FlexZBoost	2.877	<b>3.410</b>	<b>3.359</b>	0.268	<b>0.225</b>	<b>0.229</b>
	Mixture Density Network	<b>0.927</b>	<b>1.220</b>	<b>1.192</b>	<b>0.197</b>	<b>0.182</b>	<b>0.184</b>
$h = 2$	Nadaraya-Watson	<b>0.751</b>	14.47	13.14	<b>0.017</b>	0.701	0.635
	Lanne et al. (2012)	2.457	11.81	10.90	0.191	0.230	0.226
	Gourieroux and Jasiak (2025)	2.924	8.685	8.127	0.292	0.474	0.456
	FlexZBoost	2.236	<b>3.294</b>	<b>3.192</b>	0.121	<b>0.084</b>	<b>0.087</b>
	Mixture Density Network	<b>0.482</b>	<b>0.731</b>	<b>0.707</b>	<b>0.063</b>	<b>0.057</b>	<b>0.058</b>
$h = 5$	Nadaraya-Watson	<b>1.109</b>	18.23	16.58	<b>0.018</b>	0.760	0.688
	Lanne et al. (2012)	2.698	10.50	9.749	0.071	0.150	0.143
	Gourieroux and Jasiak (2025)	2.445	8.702	8.097	0.211	0.393	0.375
	FlexZBoost	1.485	<b>1.368</b>	<b>1.380</b>	0.041	<b>0.017</b>	<b>0.019</b>
	Mixture Density Network	<b>0.129</b>	<b>0.546</b>	<b>0.506</b>	<b>0.008</b>	<b>0.012</b>	<b>0.011</b>

*Notes:* This Table reports the Kullback-Leibler (KL) divergence and Integrated Squared Error (ISE) between the true predictive density and estimated densities. KL divergence measures the information loss when approximating the true distribution, while ISE quantifies the  $L^2$  distance between densities. Metrics are evaluated over three spatial regions: Center  $[q_{0.1}, q_{0.9}]$ , Tails  $[q_{0.01}, q_{0.1}] \cup [q_{0.9}, q_{0.99}]$ , and Total  $[q_{0.01}, q_{0.99}]$ , where  $q_p$  represents the  $p$ -th quantile. Best method in red, second best in bold black.

density  $p(X_{t+1} | X_t = x_i)$  across each of the three distributional regions (Center, Tails, and Total).

The MDN exhibits the lowest KL divergence and ISE in the tail region and over the full distribution across all forecast horizons. In the center of the distribution, Nadaraya-Watson remains competitive, achieving the lowest KL divergence and ISE at  $h = 1$ , and the lowest ISE at  $h = 2$ . However, it performs substantially worse for density forecasting in the tails, especially at longer horizons. At horizon  $h = 5$ , the MDN achieves a tail KL divergence of 0.546 compared to 18.23 for Nadaraya-Watson and 8.702 for Gourieroux & Jasiak (2025). Across all horizons and regions examined, the MDN consistently delivers either the best or second-best performance, demonstrating the robustness of its density forecasting capabilities.

### 3.4.2 Case 2: Predictive Moments Approach

The root mean square error (RMSE) criterion is now employed to compare the estimated conditional moments,  $\hat{\mathbb{E}}[X_{t+1}^k | X_t = x_i]$  to the theoretical ones,  $\mathbb{E}[X_{t+1}^k | X_t = x_i]$ , of Fries (2022) and measure the forecasting performance for each tail index  $\alpha \in \{1.0, 1.2, 1.4, 1.8\}$  and each moment order  $k \in \{1, 2, 3, 4\}$ , for all four DGPs in the same three regions of the distribution as in the first case-scenario. To assess the statistical significance of performance differences, we employ the Model Confidence Set (MCS) procedure of Hansen et al. (2011) with a 90% confidence level.

Note that the grid-based approach used is naturally adapted to univariate conditioning, *i.e.*, predicting  $X_{t+h}$  solely based on the current value  $X_t$ , which is consistent with the theoretical conditional moments of Fries (2022). In contrast, the forecast methods of Gourieroux & Jasiak (2025) and Lanne et al. (2012) require conditioning on multiple lags when the autoregressive order exceeds one, making direct comparison with Fries (2022)'s theoretical moments inappropriate beyond MAR(0,1) and for MARMA models. For this reason, this second-case comparative analysis is structured as follows. For the MAR(0,1) process, the MDN is compared with the full set of alternatives at all forecast horizons. For higher-order processes, MAR(0,2), MAR(1,1) and MARMA(1,1,1,1), the comparison is restricted to Nadaraya-Watson and FlexZBoost due to the conditioning set discrepancy.<sup>11</sup>

Tables 3, 4, 5, and 6 present the one-period-ahead RMSE results for all four data-generating processes. The MDN approach almost always exhibits the lowest RMSE in the tail region and over the full distribution, regardless of the tail index  $\alpha$  and the conditional

---

<sup>11</sup>Intuitively, machine learning approaches such as FlexZBoost and MDN could naturally leverage vectors of multiple past observations  $\mathbf{X}_t = (X_{t-k}, \dots, X_{t-1})^\top$  as conditioning information to improve their predictive performance. The Nadaraya-Watson estimator could also theoretically be extended to incorporate multiple conditioning lags, but at the expense of an exponential increase in computational complexity due to the curse of dimensionality (Scott 1992, Wasserman 2006), rendering it impractical for higher-dimensional conditioning sets. All alternatives could be computed in such a setup but no theoretical benchmark exists anymore. This extension is left for future work.

moment order.<sup>12</sup> In the center of the distribution, Nadaraya-Watson consistently achieves the lowest RMSE across almost all configurations, benefiting from its local averaging properties in regions where the conditional distribution exhibits more regular behavior. Importantly, when the MDN does not achieve the lowest RMSE in the center, it consistently ranks as the second-best method. The more traditional forecasting methods of Lanne et al. (2012) and Gourieroux & Jasiak (2025), as well as FlexZBoost, are almost always dominated in all regions.

Table 3: Root Mean Squared Error of Predictive Moments: MAR(0, 1) Process, 1-Step-Ahead Forecasts

Model	$\alpha$	$\mathbb{E}[y_{t+1}   y_t]$			$\mathbb{E}[y_{t+1}^2   y_t]$			$\mathbb{E}[y_{t+1}^3   y_t]$			$\mathbb{E}[y_{t+1}^4   y_t]$		
		Center	Tails	Total	Center	Tails	Total	Center	Tails	Total	Center	Tails	Total
Nadaraya-Watson	1.0	<b>0.434*</b>	43.72	41.55	<b>10.80*</b>	6619	6291	—	—	—	—	—	—
	1.2	<b>0.097*</b>	7.182	6.607	<b>1.360*</b>	341.8	314.4	<b>12.75*</b>	1.671e+04	1.538e+04	—	—	—
	1.4	<b>0.075*</b>	2.313*	2.038*	<b>0.431*</b>	49.86*	43.92*	<b>2.798*</b>	1125	991.2	—	—	—
	1.6	<b>0.047*</b>	<b>0.879</b>	<b>0.727</b>	<b>0.167*</b>	12.20	10.09	<b>0.523*</b>	149.7	123.8	<b>4.584*</b>	1786	1477
	1.8	<b>0.037*</b>	0.164	0.125*	<b>0.095*</b>	<b>1.149</b>	<b>0.863*</b>	<b>0.334*</b>	<b>6.941*</b>	<b>5.201*</b>	<b>1.642*</b>	<b>41.28*</b>	<b>30.92*</b>
Lanne et al. (2012)	1.0	1.115	39.51	37.55	133.1	7320	6956	—	—	—	—	—	—
	1.2	0.391	12.90	11.87	5.406	649.5	597.6	46.55	3.127e+04	2.877e+04	—	—	—
	1.4	0.218	4.369	3.850*	1.602	96.61	85.10	9.985	2027	1785	—	—	—
	1.6	0.121	1.010	0.838	0.679	14.71	12.17	3.171	184.1	152.3	17.51	2234	1848
	1.8	0.076	0.220	0.172	<b>0.380</b>	2.482	1.875	1.468	20.93	15.69	5.417	159.3	119.3
Gourieroux and Jasiak (2025)	1.0	4.040	19.37	18.45	81.40	<b>2666</b>	<b>2534</b>	—	—	—	—	—	—
	1.2	0.698	<b>4.649</b>	<b>4.286</b>	6.326	<b>186.1</b>	<b>171.2</b>	46.11	<b>8597</b>	<b>7910</b>	—	—	—
	1.4	0.285	<b>2.150*</b>	<b>1.898*</b>	1.590	<b>37.05*</b>	<b>32.65*</b>	6.841	<b>683.2*</b>	<b>601.9*</b>	—	—	—
	1.6	0.170	1.197	0.995	0.787	<b>11.76</b>	<b>9.736</b>	2.597	<b>123.7</b>	<b>102.3</b>	<b>11.09</b>	<b>1299</b>	<b>1075</b>
	1.8	0.092	0.449	0.342	0.385	2.526	1.908	<b>1.060</b>	15.13	11.35	<b>3.584</b>	87.15	65.28
FlexZBoost	1.0	2.107	<b>16.39</b>	<b>15.59</b>	2481	6082	5831	—	—	—	—	—	—
	1.2	0.740	4.858	4.479	98.26	482.4	445.5	332.8	4.168e+04	3.835e+04	—	—	—
	1.4	0.292	2.381*	2.102*	10.03	75.54	66.71	87.52	2221	1957	—	—	—
	1.6	0.182	1.038	0.864	1.629	18.51	15.34	9.190	318.7	263.7	89.79	5745	4751
	1.8	0.179	0.256	0.225	0.963	1.965	1.604	7.424	17.58	14.05	93.36	200.1	162.0
Mixture Density Network	1.0	<b>0.902</b>	<b>7.461*</b>	<b>7.096*</b>	<b>37.73</b>	<b>1091*</b>	<b>1037*</b>	—	—	—	—	—	—
	1.2	<b>0.305</b>	<b>1.705*</b>	<b>1.574*</b>	<b>2.980</b>	<b>67.51*</b>	<b>62.12*</b>	<b>38.00</b>	<b>2614*</b>	<b>2405*</b>	—	—	—
	1.4	<b>0.124</b>	<b>0.640*</b>	<b>0.567*</b>	0.747	<b>8.409</b>	<b>7.416</b>	4.118	<b>133.6</b>	<b>117.7</b>	—	—	—
	1.6	<b>0.082</b>	<b>0.306*</b>	<b>0.258*</b>	<b>0.427</b>	<b>2.745*</b>	<b>2.283*</b>	<b>1.932</b>	<b>31.10*</b>	<b>25.75*</b>	24.66	<b>390.1*</b>	<b>323.0*</b>
	1.8	<b>0.056</b>	<b>0.113*</b>	<b>0.093*</b>	0.421	<b>0.628*</b>	<b>0.547*</b>	1.624	<b>4.679*</b>	<b>3.664*</b>	15.36	<b>26.48*</b>	<b>22.29*</b>

*Notes:* This Table reports the root mean squared error (RMSE) of estimated predictive moments relative to theoretical values.  $\alpha$  denotes the tail index of the stable distribution. Predictive moments are evaluated over three spatial regions: Center  $[q_{0.1}, q_{0.9}]$ , Tails  $[q_{0.01}, q_{0.1}] \cup [q_{0.9}, q_{0.99}]$ , and Total  $[q_{0.01}, q_{0.99}]$ , where  $q_p$  represents the  $p$ -th quantile. Best method in red, second best in bold black. An asterisk (\*) designates model(s) which belong to the Model Confidence Set at the 90% confidence level.

The statistical significance of these performance differences is confirmed by the MCS tests. In most cases, only one forecasting approach belongs to the  $MCS_{90\%}$  set of models

<sup>12</sup>Notable exceptions occur at  $\alpha = 1.8$ : for MAR(0,2) and MAR(1,1), Nadaraya-Watson performs better for higher-order moments ( $k \geq 2$ ), while for MARMA(1,1,1,1), Nadaraya-Watson outperforms only for the fourth moment.

Table 4: Root Mean Squared Error of Predictive Moments: MAR(0, 2) Process, 1-Step-Ahead Forecasts

Model	$\alpha$	$\mathbb{E}[y_{t+1}   y_t]$			$\mathbb{E}[y_{t+1}^2   y_t]$			$\mathbb{E}[y_{t+1}^3   y_t]$			$\mathbb{E}[y_{t+1}^4   y_t]$		
		Center	Tails	Total	Center	Tails	Total	Center	Tails	Total	Center	Tails	Total
Nadaraya-Watson	1.0	<b>0.244*</b>	20.23	19.23	<b>2.252*</b>	<b>1697</b>	<b>1613</b>	—	—	—	—	—	—
	1.2	<b>0.114*</b>	5.137	4.726	<b>0.610*</b>	<b>162.9</b>	<b>149.9</b>	<b>5.464*</b>	<b>6199</b>	<b>5703</b>	—	—	—
	1.4	<b>0.086*</b>	<b>1.568</b>	<b>1.382</b>	<b>0.274*</b>	<b>21.01</b>	<b>18.51</b>	<b>0.787*</b>	<b>339.5</b>	<b>299.1</b>	—	—	—
	1.6	<b>0.044*</b>	<b>0.583</b>	<b>0.483</b>	<b>0.118*</b>	4.763	3.940	<b>0.347*</b>	<b>38.99*</b>	<b>32.25*</b>	<b>1.540*</b>	<b>368.0*</b>	<b>304.4*</b>
	1.8	<b>0.029*</b>	<b>0.188*</b>	<b>0.142*</b>	<b>0.085*</b>	<b>0.962*</b>	<b>0.722*</b>	<b>0.159*</b>	<b>4.597*</b>	<b>3.443*</b>	<b>0.578*</b>	<b>23.65*</b>	<b>17.71*</b>
FlexZBoost	1.0	1.164	<b>9.557</b>	<b>9.090</b>	617.9	1886	1803	—	—	—	—	—	—
	1.2	0.455	<b>4.648</b>	<b>4.280</b>	29.97	226.7	208.9	59.39	1.322e+04	1.216e+04	—	—	—
	1.4	0.265	1.789	1.581	3.475	39.33	34.68	19.30	1070	942.4	—	—	—
	1.6	0.200	0.695	0.586	1.345	<b>4.626</b>	<b>3.900</b>	12.98	47.36	39.85	226.6	502.1	434.4
	1.8	0.187	0.267	0.235	0.703	1.092	0.941	3.668	9.215	7.315	32.50	72.83	58.63
Mixture Density Network	1.0	<b>0.733</b>	<b>5.713*</b>	<b>5.435*</b>	<b>21.11</b>	<b>291.6*</b>	<b>277.2*</b>	—	—	—	—	—	—
	1.2	<b>0.129*</b>	<b>2.285*</b>	<b>2.103*</b>	<b>1.647</b>	<b>41.24*</b>	<b>37.94*</b>	<b>41.53</b>	<b>2067*</b>	<b>1902*</b>	—	—	—
	1.4	<b>0.084*</b>	<b>0.607*</b>	<b>0.536*</b>	<b>0.773</b>	<b>8.158*</b>	<b>7.196*</b>	<b>2.672</b>	<b>161.3*</b>	<b>142.1*</b>	—	—	—
	1.6	<b>0.084</b>	<b>0.276*</b>	<b>0.233*</b>	<b>0.575</b>	<b>2.696*</b>	<b>2.253*</b>	<b>2.873</b>	<b>28.51*</b>	<b>23.63*</b>	<b>30.92</b>	<b>309.6*</b>	<b>256.6*</b>
	1.8	<b>0.049</b>	<b>0.168*</b>	<b>0.130*</b>	<b>0.345</b>	<b>1.032*</b>	<b>0.806</b>	<b>1.053</b>	<b>6.553</b>	<b>4.955</b>	<b>8.499</b>	<b>59.19</b>	<b>44.66</b>

Notes: For details on variable definitions and methodology, refer to Table 3. An asterisk (\*) designates model(s) which belong to the Model Confidence Set at the 90% confidence level.

Table 5: Root Mean Squared Error of Predictive Moments: MAR(1, 1) Process, 1-Step-Ahead Forecasts

Model	$\alpha$	$\mathbb{E}[y_{t+1}   y_t]$			$\mathbb{E}[y_{t+1}^2   y_t]$			$\mathbb{E}[y_{t+1}^3   y_t]$			$\mathbb{E}[y_{t+1}^4   y_t]$		
		Center	Tails	Total	Center	Tails	Total	Center	Tails	Total	Center	Tails	Total
Nadaraya-Watson	1.0	<b>0.506*</b>	40.06	38.07	<b>13.94*</b>	<b>7557</b>	<b>7182</b>	—	—	—	—	—	—
	1.2	<b>0.104*</b>	6.755	6.215	<b>1.469*</b>	<b>378.8</b>	<b>348.5</b>	<b>16.37*</b>	<b>2.040e+04</b>	<b>1.877e+04</b>	—	—	—
	1.4	<b>0.083*</b>	2.312	2.037	<b>0.566*</b>	<b>59.61</b>	<b>52.51</b>	<b>4.169*</b>	<b>1513</b>	<b>1333</b>	—	—	—
	1.6	<b>0.047*</b>	<b>0.798</b>	<b>0.660</b>	<b>0.199*</b>	<b>12.24</b>	<b>10.12</b>	<b>0.688*</b>	<b>170.4</b>	<b>140.9</b>	<b>5.156*</b>	<b>2312</b>	<b>1912</b>
	1.8	<b>0.040*</b>	<b>0.159*</b>	<b>0.122*</b>	<b>0.113*</b>	<b>1.335*</b>	<b>1.002*</b>	<b>0.428*</b>	<b>9.769*</b>	<b>7.319*</b>	<b>2.135*</b>	<b>70.68*</b>	<b>52.93*</b>
FlexZBoost	1.0	2.320	<b>17.85</b>	<b>16.98</b>	3065	7661	7343	—	—	—	—	—	—
	1.2	0.791	<b>5.266</b>	<b>4.855</b>	120.7	616.9	569.5	462.4	5.894e+04	5.423e+04	—	—	—
	1.4	0.349	<b>2.174</b>	<b>1.922</b>	12.40	84.16	74.37	120.5	2932	2583	—	—	—
	1.6	0.191	1.306	1.086	1.996	27.51	22.78	12.41	529.1	437.6	119.7	1.049e+04	8678
	1.8	0.194	0.353	0.294	1.015	3.798	2.922	8.195	38.76	29.52	108.6	424.0	325.5
Mixture Density Network	1.0	<b>0.967</b>	<b>3.751*</b>	<b>3.578*</b>	<b>47.44</b>	<b>863.9*</b>	<b>821.2*</b>	—	—	—	—	—	—
	1.2	0.328	<b>1.789*</b>	<b>1.651*</b>	4.245	<b>86.04*</b>	<b>79.17*</b>	62.46	<b>3998*</b>	<b>3678*</b>	—	—	—
	1.4	0.094*	<b>1.021*</b>	<b>0.901*</b>	0.844	<b>19.21*</b>	<b>16.92*</b>	4.898	<b>367.2*</b>	<b>323.5*</b>	—	—	—
	1.6	0.061*	<b>0.302*</b>	<b>0.252*</b>	0.479	<b>2.472*</b>	<b>2.062*</b>	2.441	<b>23.10*</b>	<b>19.16*</b>	<b>31.12</b>	<b>300.8*</b>	<b>249.4*</b>
	1.8	0.067	<b>0.154*</b>	<b>0.123*</b>	0.467	<b>1.367*</b>	<b>1.069*</b>	1.927	<b>12.52*</b>	9.462*	18.88	118.4	89.51

Notes: For details on variable definitions and methodology, refer to Table 3. An asterisk (\*) designates model(s) which belong to the Model Confidence Set at the 90% confidence level.

Table 6: Root Mean Squared Error of Predictive Moments: MARMA(1, 1, 1, 1) Process, 1-Step-Ahead Forecasts

Model	$\alpha$	$\mathbb{E}[y_{t+1}   y_t]$			$\mathbb{E}[y_{t+1}^2   y_t]$			$\mathbb{E}[y_{t+1}^3   y_t]$			$\mathbb{E}[y_{t+1}^4   y_t]$		
		Center	Tails	Total	Center	Tails	Total	Center	Tails	Total	Center	Tails	Total
Nadaraya-Watson	1.0	<b>0.711*</b>	41.50	39.44	<b>27.39*</b>	<b>3236</b>	<b>3076</b>	—	—	—	—	—	—
	1.2	<b>0.134*</b>	6.808	6.264	<b>1.149*</b>	<b>194.5</b>	<b>178.9</b>	<b>26.24*</b>	<b>8876</b>	<b>8166</b>	—	—	—
	1.4	<b>0.082*</b>	2.129	1.876	<b>0.383*</b>	<b>42.68</b>	<b>37.59</b>	<b>3.275*</b>	<b>1044</b>	<b>919.7</b>	—	—	—
	1.6	<b>0.056*</b>	<b>0.478*</b>	<b>0.396*</b>	<b>0.127*</b>	4.996	4.132	<b>0.984*</b>	<b>46.74</b>	<b>38.66*</b>	<b>10.97*</b>	<b>631.4</b>	<b>522.2</b>
	1.8	<b>0.042*</b>	<b>0.290</b>	<b>0.219*</b>	<b>0.116*</b>	<b>1.566</b>	<b>1.175*</b>	<b>0.207*</b>	<b>9.357*</b>	<b>7.006*</b>	<b>1.216*</b>	<b>48.67*</b>	<b>36.44*</b>
FlexZBoost	1.0	1.679	<b>20.73</b>	<b>19.71</b>	1770	6375	6083	—	—	—	—	—	—
	1.2	0.592	<b>4.634</b>	<b>4.269</b>	66.67	344.6	318.1	185.0	4.014e+04	3.693e+04	—	—	—
	1.4	0.296	<b>1.736</b>	<b>1.536</b>	6.192	68.48	60.39	40.52	2015	1775	—	—	—
	1.6	0.201	0.828	0.694	1.488	19.57	16.21	11.53	277.7	229.8	185.3	8553	7074
	1.8	0.196	0.402	0.328	0.693	4.325	3.270	4.234	38.92	29.27	43.93	426.0	320.2
Mixture Density Network	1.0	<b>0.689*</b>	<b>5.908*</b>	<b>5.619*</b>	<b>68.94</b>	<b>659.3*</b>	<b>626.9*</b>	—	—	—	—	—	—
	1.2	<b>0.261</b>	<b>2.209*</b>	<b>2.035*</b>	1.493	<b>23.46*</b>	<b>21.59*</b>	42.15	<b>1805*</b>	<b>1661*</b>	—	—	—
	1.4	<b>0.173</b>	<b>0.925*</b>	<b>0.819*</b>	1.186	<b>4.344*</b>	<b>3.868*</b>	13.60	<b>180.8*</b>	<b>159.4*</b>	—	—	—
	1.6	<b>0.086</b>	<b>0.327*</b>	<b>0.274*</b>	0.633	<b>0.972*</b>	<b>0.879*</b>	3.186	<b>26.41*</b>	<b>21.91*</b>	41.99	<b>180.3*</b>	<b>151.0*</b>
	1.8	<b>0.089</b>	<b>0.132*</b>	<b>0.115*</b>	0.576	<b>0.902*</b>	<b>0.776*</b>	2.915	<b>6.460*</b>	<b>5.208*</b>	22.14	52.50*	41.95

Notes: For details on variable definitions and methodology, refer to Table 3.

with superior forecasting abilities: Nadaraya-Watson for the central region, and the MDN for the tail region and overall distribution.<sup>13</sup>

<sup>13</sup>We also test the sensitivity of our findings to the choice of the forecast horizon ( $h = 2$  and  $h = 5$ ) both in terms of RMSE and MCS test. The results, available in Section 3 of the Online Appendix, are qualitatively similar.

Figure 3 provides a visual comparison of the one-step-ahead predictive conditional moments for a  $\text{MAR}(0,1)$  process with tail-index  $\alpha = 1.4$  across the five competing approaches. The MDN produces smooth predictions that closely track the theoretical moments throughout the distribution. Gourieroux & Jasiak (2025)'s forecasts are also smooth but increasingly drift from the truth in the tails. FlexZBoost exhibits a staircase-like pattern with systematic deviations. The moment forecasts from Nadaraya-Watson and Lanne et al. (2012) become increasingly noisy as we move away from the center. These patterns are qualitatively similar, though noisier, at longer horizons  $h = 2$  and  $h = 5$  (see the Online Appendix).

### 3.4.3 Case 3: Comparison with the Realized Outcomes

Rather than evaluating predictive densities at pre-specified conditioning values, we now train each method on 5,000 observations from a  $\text{MAR}(0,1)$  process and use the trained models to forecast the subsequent 500 realizations. This approach allows us to assess density forecast quality using proper scoring rules that directly compare the predictive density,  $\hat{p}(X_{t+1} | X_t = x_i)$ , against the realized outcome  $X_{t+1}$ .

Table 7 presents detailed results for forecast horizons  $h \in \{1, 2, 5\}$  using four complementary evaluation metrics: the Conditional Density Estimation (CDE) loss, the Continuous Ranked Probability Score (CRPS), the logarithmic probability score, and the quantile score at the 10% level.<sup>14</sup> As in our previous evaluation strategy, we assess the performance across three distributional regions (Center, Tails, and Total) to capture method-specific strengths. The results corroborate our grid-based findings. At the one-step-ahead horizon, the MDN achieves the best or second-best performance across nearly all metrics and tail index values, and it is particularly excelling in the tail region. As the forecast horizon

---

<sup>14</sup>For CDE loss, CRPS, and quantile scores, lower values indicate superior performance, while for the log probability score, higher values are preferred.

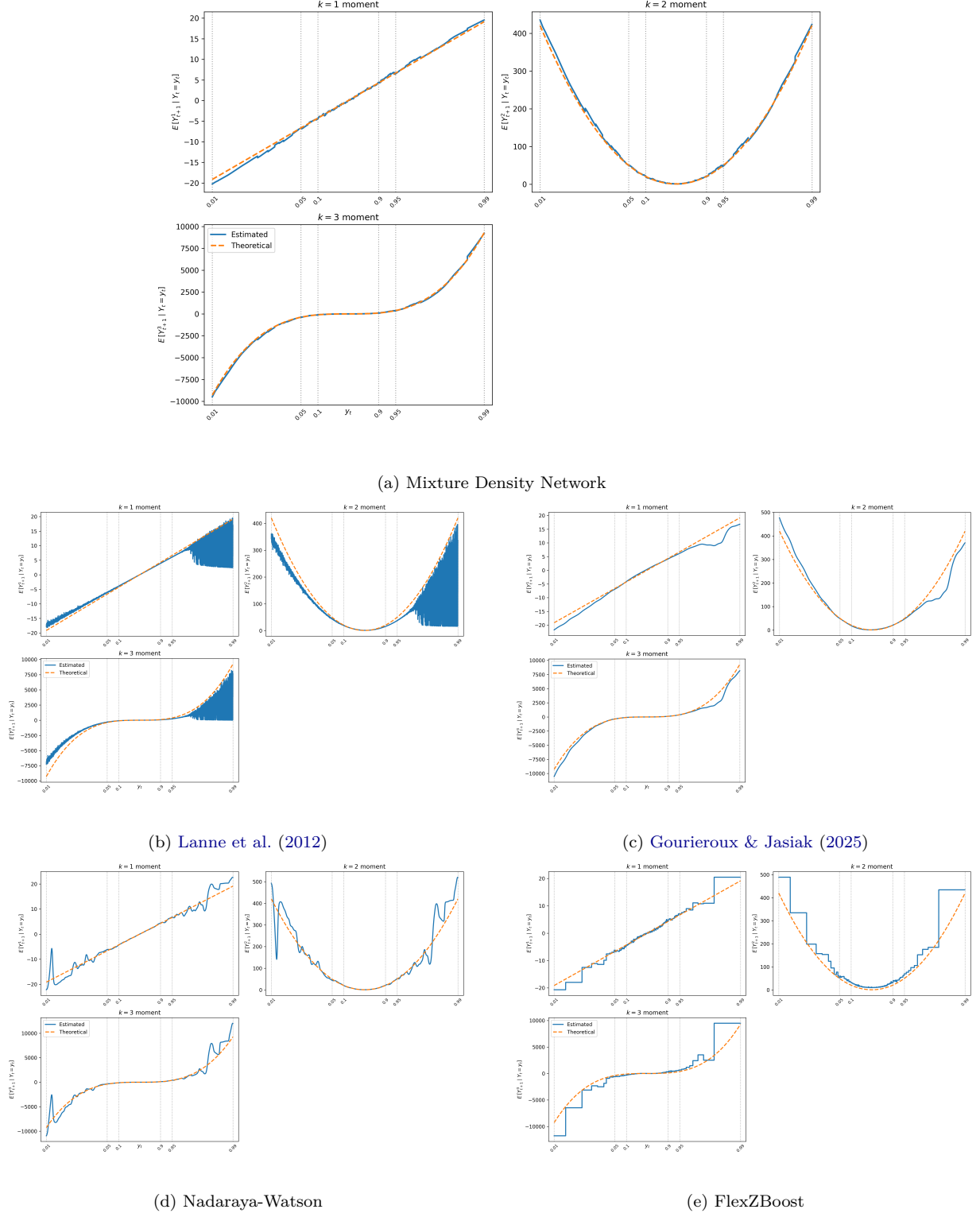


Figure 3: Conditional Predictive Moment Accuracy: MAR(0,1) Process, 1-Step-Ahead Forecasts

*Notes:* This figure displays the estimated predictive moments  $\mathbb{E}[y_{t+1}^k | y_t]$  for  $k \in \{1, 2, 3\}$  as a function of the conditioning variable  $y_t$  for a purely noncausal MAR(0,1) process with  $\alpha$ -stable innovations. Each panel from (a) to (e) shows the results for a specific density forecasting method. Blue curves represent estimated moments, while orange curves show the corresponding theoretical ones. The tail-index is fixed at  $\alpha = 1.4$ .

extends to  $h = \{2, 5\}$ , the relative performance rankings remain remarkably stable. The MDN continues to dominate in the tail region and overall distribution for most  $\alpha$  values, though Nadaraya-Watson exhibits competitive performance for  $\alpha = 1.8$ , in particular at longer horizons. This pattern suggests that kernel-based methods can perform well when the DGP approaches a Gaussian one, but struggle with heavier tails where the MDN's flexible mixture components provide clear advantages. Note also that contrary to the previous two

Table 7: Density Forecast Performance Metrics: MAR(0, 1) Process, 1-Step-Ahead Forecasts

Model	$\alpha$	CDE Loss			CRPS			Log Prob			QS 10%			
		Center	Tails	Total	Center	Tails	Total	Center	Tails	Total	Center	Tails	Total	
Nadaraya-Watson Lanne et al. (2012)	1.0	<b>-0.235</b>	<b>-0.076</b>	<b>-0.221</b>	<b>1.217</b>	<b>3.716</b>	<b>2.041</b>	<b>-2.354</b>	-4.824	<b>-2.822</b>	<b>0.509</b>	1.964	<b>0.889</b>	
		0.161	0.080	0.135	3.499	3.811	3.794	-3.926	<b>-3.882</b>	-4.207	0.702	<b>0.756</b>	<b>0.841</b>	
		0.144	0.192	0.172	3.709	4.312	4.402	-4.046	-4.976	-4.450	1.522	1.916	1.779	
		-0.034	-0.014	-0.011	7.363	12.13	10.71	-3.452	-4.511	-4.785	1.167	5.739	5.476	
		<b>-0.098</b>	<b>-0.087</b>	<b>-0.088</b>	<b>1.584</b>	<b>2.817</b>	<b>2.281</b>	<b>-2.568</b>	<b>-2.887</b>	<b>-2.773</b>	<b>0.693</b>	<b>0.965</b>	0.942	
Nadaraya-Watson Lanne et al. (2012)	1.2	<b>-0.308</b>	<b>-0.342</b>	<b>-0.299</b>	<b>0.690</b>	<b>1.126</b>	<b>0.993</b>	<b>-1.750</b>	<b>-2.158</b>	<b>-1.927</b>	<b>0.264</b>	<b>0.296</b>	<b>0.299</b>	
		-0.129	-0.130	-0.114	0.834	1.435	1.128	-2.029	-3.273	-2.403	0.272	0.432	0.342	
		0.029	-0.085	-0.015	0.988	1.325	1.296	-2.236	-2.307	-2.429	0.297	0.309	0.335	
		-0.081	-0.076	-0.051	1.685	2.896	2.440	-2.585	-3.014	-3.228	0.552	1.132	1.141	
		<b>-0.302</b>	<b>-0.348</b>	<b>-0.290</b>	<b>0.682</b>	<b>1.108</b>	<b>0.996</b>	<b>-1.580</b>	<b>-1.600</b>	<b>-1.710</b>	<b>0.258</b>	<b>0.288</b>	<b>0.334</b>	
Nadaraya-Watson Lanne et al. (2012)	1.4	<b>-0.350</b>	<b>-0.486</b>	<b>-0.327</b>	<b>0.511</b>	<b>0.585</b>	<b>0.703</b>	<b>-1.397</b>	<b>-1.151</b>	<b>-1.582</b>	<b>0.161</b>	<b>0.167</b>	<b>0.201</b>	
		-0.288	-0.459	-0.258	0.529	0.752	0.721	-1.418	-1.663	-1.765	0.166	0.266	0.223	
		0.027	-0.237	-0.408	-0.207	0.583	0.587	0.770	-1.503	-1.329	-1.750	0.175	0.173	0.210
		-0.184	-0.237	-0.149	0.795	0.927	0.965	-1.982	-1.846	-2.266	0.279	0.325	0.390	
		<b>-0.355</b>	<b>-0.542</b>	<b>-0.332</b>	<b>0.511</b>	<b>0.585</b>	<b>0.684</b>	<b>-1.266</b>	<b>-1.037</b>	<b>-1.450</b>	<b>0.160</b>	<b>0.166</b>	<b>0.202</b>	
Nadaraya-Watson Lanne et al. (2012)	1.6	<b>-0.398</b>	<b>-0.608</b>	<b>-0.360</b>	0.432	<b>0.350</b>	<b>0.514</b>	<b>-1.149</b>	<b>-0.796</b>	<b>-1.317</b>	<b>0.127</b>	<b>0.104</b>	<b>0.152</b>	
		-0.388	-0.444	-0.301	<b>0.427</b>	0.420	0.540	-1.156	-1.506	-1.522	0.128	0.121	0.162	
		0.030	-0.513	-0.280	0.467	0.386	0.569	-1.244	-0.940	-1.470	0.138	0.105	0.163	
		-0.354	-0.492	-0.298	0.452	0.393	0.558	-1.542	-0.944	-1.673	0.145	0.125	0.182	
		<b>-0.410</b>	<b>-0.578</b>	<b>-0.356</b>	<b>0.420</b>	<b>0.359</b>	<b>0.529</b>	<b>-1.083</b>	<b>-0.834</b>	<b>-1.288</b>	<b>0.125</b>	<b>0.105</b>	<b>0.159</b>	
Nadaraya-Watson Lanne et al. (2012)	1.8	<b>-0.455</b>	<b>-0.716</b>	<b>-0.386</b>	0.371	<b>0.262</b>	<b>0.437</b>	<b>-0.971</b>	<b>-0.535</b>	<b>-1.164</b>	<b>0.109</b>	0.078	<b>0.130</b>	
		-0.416	-0.411	-0.327	<b>0.370</b>	0.295	0.440	-1.005	-1.044	-1.357	0.110	0.080	0.131	
		0.045	<b>-0.706</b>	-0.357	0.384	0.264	0.450	-1.037	<b>-0.539</b>	-1.240	0.111	<b>0.077</b>	0.136	
		-0.434	-0.657	-0.378	0.381	0.281	0.447	-1.588	-1.336	-1.787	0.109	0.089	0.131	
		<b>-0.460</b>	-0.687	<b>-0.382</b>	<b>0.368</b>	<b>0.263</b>	<b>0.434</b>	<b>-0.943</b>	-0.571	<b>-1.152</b>	<b>0.107</b>	<b>0.075</b>	<b>0.128</b>	

*Notes:* This table reports density forecast performance metrics across different tail index values ( $\alpha$ ). CDE Loss (Conditional Density Estimation loss), CRPS (Continuous Ranked Probability Score), and QS 10% (Quantile Score at 10% level) are loss functions where lower values indicate better performance. Log Prob (Log Probability Score) is a scoring rule where higher values indicate better performance. Metrics are evaluated over three spatial regions: Center  $[q_{0.1}, q_{0.9}]$ , Tails  $[q_{0.01}, q_{0.1}] \cup [q_{0.9}, q_{0.99}]$ , and Total  $[q_{0.01}, q_{0.99}]$ , where  $q_p$  represents the  $p$ -th quantile. Best method in red, second best in bold black.

setups, this evaluation framework has the advantage of allowing one to compare all the alternative forecasting approaches for all MAR models and at all forecast horizons.

As a final remark, comparing Tables 2 and 7 for the  $\alpha = 1.0$  case reveals a notable discrepancy. When evaluated against the true predictive density, the MDN exhibits clear dominance, achieving KL divergence and ISE values substantially lower than all competitors both in the tail and over the total regions. However, when assessed using proxy metrics that do not require the true density, although the MDN remains among the best-performing

methods, its superiority is far less apparent. This suggests that standard scoring rules may lack sufficient discriminatory power to identify the best-performing forecasting method when predictive distributions exhibit heavy tails and bimodality.

### 3.5 Runtime Analysis

Finally, Table 8 reports the average computational time (over all tail indices  $\alpha$ ) required by each method to generate the forecasts for a MAR(0,1) process. For each forecast horizon, the reported runtime corresponds to the average time needed to compute the 5,000 conditional predictive densities over the grid of conditioning values  $\{x_1, \dots, x_{5000}\}$ . FlexZBoost achieves the shortest runtime (under 5 seconds), though at the cost of inferior forecast accuracy, as demonstrated above. The MDN requires only 2-3 minutes. In stark contrast, the simulation-based methods of [Lanne et al. \(2012\)](#) and [Gourieroux & Jasiak \(2025\)](#) require substantially longer computation times, with the latter exhibiting a dramatic increase from about 1 hour at  $h = 1$  to over 5 hours at  $h = 5$ .

Model	Horizon 1	Horizon 2	Horizon 5
Nadaraya-Watson	9.38	9.34	10.72
<a href="#">Gourieroux &amp; Jasiak (2025)</a>	59.03	117.85	300.54
<a href="#">Lanne et al. (2012)</a>	106.33	107.37	107.69
FlexZBoost	0.04	0.05	0.05
Mixture Density Network	2.64	2.20	1.92

Table 8: Average running time (in minutes)

## 4 Forecasting Natural Gas Prices in Real Time

Having established the MDN’s superior performance in controlled simulation settings where the true DGP is known, we now evaluate its forecasting ability on real-world data where model specification uncertainty and data complexities are unavoidable. Natural gas prices

are notoriously difficult to forecast due to the interplay of supply-side fundamentals, weather-driven demand shocks, and periodic episodes of locally explosive behavior stemming from infrastructure bottlenecks or extreme weather events (Baumeister et al. 2025). These characteristics make the natural gas market a compelling testbed for our MDN approach.

We adopt the real-time forecasting framework of Baumeister et al. (2025), who provide an extensive evaluation of point forecasting methods for the real Henry Hub spot price – the benchmark for North American natural gas markets. Their setup accounts for publication lags and data revisions through a comprehensive database of monthly vintages, ensuring that forecasts rely only on information available at each forecast origin. The estimation period runs from January 1976 to January 1997, and the out-of-sample evaluation period spans February 1997 to February 2024. We use forecast horizons  $h$  ranging from 1 to 24 months. We defer the reader to Baumeister et al. (2025) for a detailed description of the data construction and real-time constraints.

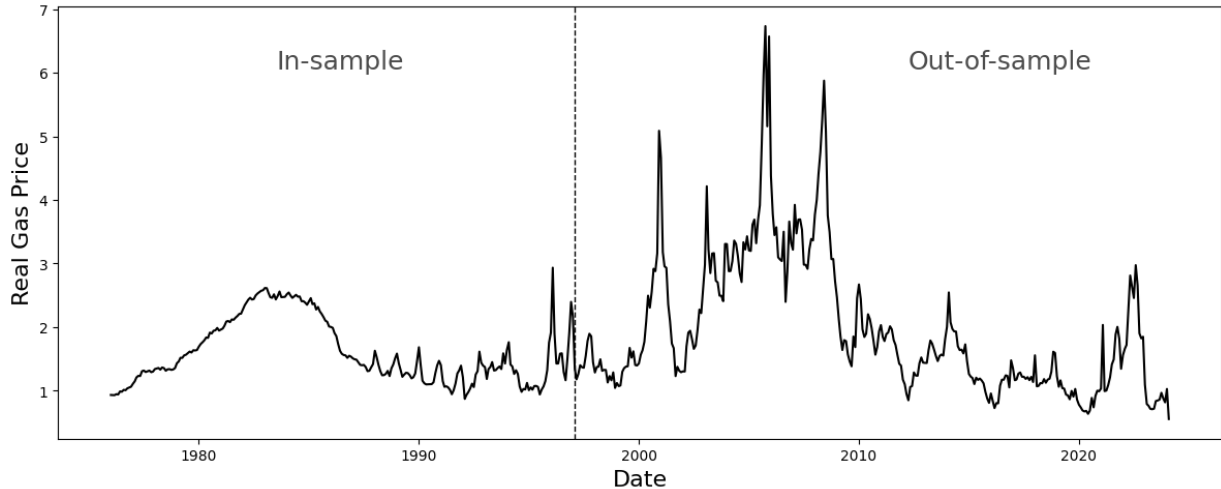


Figure 4: Real Henry Hub spot price of natural gas.

Figure 4 displays the evolution of the real Henry Hub spot price over the sample period. The series exhibits clear episodes of locally explosive behavior, most notably during the 2005-2008 and the 2021-2022 periods, characterized by sharp run-ups followed by abrupt collapses, precisely the type of dynamics that noncausal processes are designed to capture.

Using the GCov estimation method (Gourieroux & Jasiak 2023) on the in-sample period (1976M1-1997M1), we estimate all possible MAR( $p, q$ ) specifications such that  $p + q \leq k$ , where  $k$  is chosen based on the Autocorrelation and Partial Autocorrelation Functions. Then we select the model yielding i.i.d. residuals based on the portmanteau test of Jasiak & Neyazi (2025). The best specification is a purely noncausal MAR(0,1) process. The  $\alpha$ -stable distribution parameters and their respective standard deviations are then obtained by fitting the characteristic function-based estimator of Nolan (2020) to the filtered residuals.<sup>15</sup> Importantly, applying the same procedure to the full post-revised series (1976M1–2024M2), one also finds that the MAR(0,1) specification is the best model. The parameter estimates are comparable, which confirms the robustness and temporal stability of the noncausal process dynamics.

As reported in Table 9, both samples reveal strong anticipative persistence ( $\hat{\psi} \approx 0.95$ ) and heavy tails ( $\hat{\alpha} \approx 1.8$ ), substantially thicker than in the Gaussian case ( $\alpha = 2$ ), and consistent with the extreme price movements observed in the data.

Table 9: Estimated MAR(0,1) parameters for the real Henry Hub spot price

Parameter	Real-Time In-Sample	Full Period Post-Revised
$\psi$	0.957*** (0.018)	0.945*** (0.015)
$\alpha$	1.779*** (0.186)	1.830*** (0.125)
$\beta$	0.415** (0.200)	0.628*** (0.149)
$\sigma$	0.070*** (0.006)	0.158*** (0.009)

Standard errors in parentheses. \*\*\*  $p < 0.01$ , \*\*  $p < 0.05$ , \*  $p < 0.10$

To evaluate the density forecasting performance of our MDN approach in this real-time setting, we simulate a trajectory of 5,000 observations based on the parameters of the estimated MAR(0,1) process reported in Table 9 and train the five density forecasting methods on this simulated data. Once trained, each method produces density forecasts for the entire out-of-sample period (1997M2–2024M2) at  $h \in \{1, 3, 6, 9, 12, 15, 18, 21, 24\}$

---

<sup>15</sup>The standard deviations of the MAR parameters are obtained following Gourieroux & Jasiak (2023).

months ahead. We assess the quality of the predictive densities with the four complementary metrics used in simulations (CDE loss, CRPS, log-probability score, quantile score).

Table 10 summarizes the results. The MDN approach delivers the best or near-best performance across the majority of horizons and metrics. At the shortest horizon ( $h = 1$ ), the MDN achieves the best CDE loss and CRPS, while FlexZBoost achieves a slightly lower quantile score. The MDN dominates in terms of log-probability score across all horizons. From  $h = 3$  onward, the MDN consistently achieves the best performance across all four metrics, with only occasional exceptions at intermediate horizons ( $h = 12, 15$ ) where Nadaraya-Watson performs marginally better in terms of CDE loss and CRPS. Importantly, when the MDN is not the best performer for a given metric, it consistently ranks as the second-best method. A natural question is whether the MDN’s well-calibrated predictive distributions also translate into accurate point predictions. Table 11 addresses this by comparing the Mean Squared Prediction Error (MSPE) of the MDN’s point forecasts, computed as the median of the predictive density, against the forecasts of a comprehensive set of models evaluated by Baumeister et al. (2025), expressed as ratios relative to the no-change benchmark, *i.e.*, the current price. The comparison encompasses both univariate specifications (AR(1), AR(AIC), exponential smoothing) and multivariate Bayesian VAR models that incorporate additional predictors such as oil prices, industrial production, and storage levels.

The MDN delivers the lowest MSPE at all horizons from  $h = 1$  to  $h = 9$ , outperforming not only simple univariate specifications but also the economically-motivated BVAR models that Baumeister et al. (2025) identify as top performers. At the 9-month horizon, the MDN achieves an MSPE ratio of 0.746, *i.e.* a 25% improvement over the random walk and substantially better than the next best competitor, the BVAR(1), which registers a ratio of 0.804. At longer horizons ( $h \geq 12$ ), the BVAR(1) takes the lead, while the exponential

Table 10: Density forecast comparison

Horizon	Metric	Nadaraya-Watson	Lanne et al. (2012)	Gourieroux and Jasiak (2025)	FlexZBoost	Mixture Density Network
$h = 1$	CDE loss	-0.990	8.105	-0.631	<b>-1.130</b>	<b>-1.167</b>
	CRPS	0.189	0.212	0.195	<b>0.177</b>	<b>0.175</b>
	Log probability score	<b>-0.453</b>	-8.463	-0.710	-1.165	<b>-0.214</b>
	Quantile score (10%)	<b>0.062</b>	0.078	0.093	<b>0.059</b>	0.063
$h = 3$	CDE loss	<b>-0.660</b>	7.813	0.881	-0.637	<b>-0.701</b>
	CRPS	0.311	0.395	0.392	<b>0.297</b>	<b>0.291</b>
	Log probability score	<b>-1.024</b>	-8.839	-2.375	-3.573	<b>-0.713</b>
	Quantile score (10%)	0.099	0.174	0.235	<b>0.090</b>	<b>0.081</b>
$h = 6$	CDE loss	<b>-0.506</b>	9.300	1.530	-0.469	<b>-0.542</b>
	CRPS	0.432	0.613	0.628	<b>0.410</b>	<b>0.393</b>
	Log probability score	<b>-1.416</b>	-9.429	-3.645	-3.904	<b>-1.029</b>
	Quantile score (10%)	0.144	0.217	0.426	<b>0.120</b>	<b>0.118</b>
$h = 9$	CDE loss	<b>-0.446</b>	9.128	1.615	-0.383	<b>-0.459</b>
	CRPS	0.468	0.790	0.781	<b>0.453</b>	<b>0.435</b>
	Log probability score	<b>-1.440</b>	-10.90	-4.083	-3.906	<b>-1.102</b>
	Quantile score (10%)	<b>0.137</b>	0.254	0.564	0.145	<b>0.116</b>
$h = 12$	CDE loss	<b>-0.404</b>	9.744	2.062	-0.350	<b>-0.402</b>
	CRPS	<b>0.474</b>	0.950	0.960	<b>0.474</b>	0.478
	Log probability score	<b>-1.519</b>	-11.17	-4.767	-3.625	<b>-1.232</b>
	Quantile score (10%)	<b>0.119</b>	0.234	0.724	0.128	<b>0.117</b>
$h = 15$	CDE loss	<b>-0.354</b>	10.14	2.195	-0.283	<b>-0.348</b>
	CRPS	<b>0.489</b>	1.067	1.181	0.511	<b>0.510</b>
	Log probability score	<b>-1.669</b>	-11.32	-5.064	-4.285	<b>-1.327</b>
	Quantile score (10%)	<b>0.120</b>	0.223	0.937	0.134	<b>0.117</b>
$h = 18$	CDE loss	<b>-0.332</b>	11.06	2.242	-0.244	<b>-0.349</b>
	CRPS	<b>0.514</b>	1.165	1.318	0.533	<b>0.515</b>
	Log probability score	<b>-1.766</b>	-12.14	-5.149	-4.773	<b>-1.350</b>
	Quantile score (10%)	<b>0.122</b>	0.227	1.043	0.136	<b>0.114</b>
$h = 21$	CDE loss	<b>-0.341</b>	9.754	2.085	-0.273	<b>-0.356</b>
	CRPS	<b>0.524</b>	1.255	1.359	0.552	<b>0.516</b>
	Log probability score	<b>-1.748</b>	-11.67	-5.026	-4.682	<b>-1.339</b>
	Quantile score (10%)	<b>0.120</b>	0.230	1.005	0.134	<b>0.115</b>
$h = 24$	CDE loss	<b>-0.336</b>	9.564	2.143	-0.245	<b>-0.336</b>
	CRPS	<b>0.532</b>	1.342	1.408	0.564	<b>0.524</b>
	Log probability score	<b>-1.780</b>	-12.65	-5.280	-4.307	<b>-1.359</b>
	Quantile score (10%)	<b>0.117</b>	0.231	0.986	0.133	<b>0.109</b>

Best method in red, second best in bold black.

smoothing dominates at  $h \geq 21$  although the MDN remains competitive, consistently ranking second-best among all competing methods at horizons  $h = 12, 18, 21, 24$ . These results are particularly remarkable given that the MDN relies solely on the univariate price history, whereas the BVAR models exploit a rich information set of macroeconomic and energy market variables. Moreover, unlike [Baumeister et al. \(2025\)](#), our approach does not require recursive re-estimation of the model at each forecast origin, making it computationally more efficient.

The excellent point forecast performance of the MDN can be partly attributed to the noncausal specification itself. By explicitly modeling the anticipative dynamics, the MAR(0,1) process captures the locally explosive behavior of natural gas prices, a feature

Table 11: Average MSPE Ratios Relative to the No-Change Forecast of the Real Natural Gas Spot Price

Horizon	Univariate Models			Multivariate Models		Mixture Density Network
	AR(1)	AR(AIC)	Exp. Smoothing	BVAR(AIC)	BVAR(1)	
1	0.987	1.043	2.120	1.006	<b>0.969</b>	<b>0.928</b>
3	0.956	0.978	1.257	0.972	<b>0.926</b>	<b>0.878</b>
6	0.900	0.891	0.941	0.898	<b>0.852</b>	<b>0.799</b>
9	0.855	0.849	0.819	0.827	<b>0.804</b>	<b>0.746</b>
12	0.837	0.827	0.798	0.810	<b>0.766</b>	<b>0.778</b>
15	0.836	0.825	<b>0.802</b>	0.827	<b>0.767</b>	0.808
18	0.843	0.830	0.808	0.852	<b>0.785</b>	<b>0.805</b>
21	0.853	0.836	<b>0.792</b>	0.856	0.819	<b>0.813</b>
24	0.871	0.844	<b>0.782</b>	0.883	0.850	<b>0.825</b>

Values below 1 indicate improvements relative to the no-change forecast. Best method in red, second best in bold black.

that the purely causal models employed by Baumeister et al. (2025) cannot accommodate. Furthermore, the MDN outperforms the alternative density forecasting methods in terms of MSPE. Detailed results are reported in the Online Appendix.

## 5 Conclusion

Forecasting time series that exhibit locally explosive behavior, characterized by sharp run-ups followed by abrupt collapses, remains a fundamental challenge in financial econometrics. While mixed causal-noncausal autoregressive models have emerged as theoretically appealing frameworks for capturing such dynamics, their practical implementation for forecasting has been hindered by the absence of closed-form predictive densities and the computational burden of simulation-based alternatives. This paper addresses these challenges by proposing a Mixture Density Network specifically tailored to the distributional properties of noncausal processes. Our approach combines skewed t-distribution mixture components with an adaptive weighting scheme that emphasizes tail observations during training, followed by post-hoc recalibration to correct for the induced distributional shift. This architecture enables near-instantaneous density forecasts once trained, circumventing the computational limitations of existing methods.

We evaluate our approach through extensive Monte Carlo simulations that cover a range of MARMA specifications. The results show that the MDN method consistently achieves the best performances in the tail regions and over the full distribution at all forecast horizons. An empirical application to real-time forecasting of natural gas prices further validates these findings: the MDN delivers superior density forecasts, and it achieves the lowest MSPE at horizons up to 9 months ahead. Most importantly, it outperforms both univariate benchmarks and multivariate BVAR models.

## References

Avelino, J. G., Cavalcanti, G. D. C. & Cruz, R. M. O. (2024), 'Resampling strategies for imbalanced regression: A survey and empirical analysis', *Artificial Intelligence Review* **57**(4), 82.

Azzalini, A. & Dalla Valle, A. (1996), 'The multivariate skew-normal distribution', *Biometrika* **83**(4), 715–726.

Baumeister, C., Huber, F., Lee, T. K. & Ravazzolo, F. (2025), 'Forecasting natural gas prices in real time', *Journal of Applied Econometrics* .

Bishop, C. M. (1994), 'Mixture density networks'.

Blasques, F., Koopman, S. J., Mingoli, G. & Telg, S. (2025), 'A novel test for the presence of local explosive dynamics', *Journal of Time Series Analysis* .

Branco, P., Torgo, L. & Ribeiro, R. P. (2019), 'Pre-processing approaches for imbalanced distributions in regression', *Neurocomputing* **343**, 76–99.

Bruffaerts, C., Verardi, V. & Vermandele, C. (2014), 'A generalized boxplot for skewed and heavy-tailed distributions', *Statistics & Probability Letters* **95**, 110–117.

Castle, J., Hendry, D. F. & Clements, M. P. (2019), *Forecasting*, Yale University Press.

Cavaliere, G., Nielsen, H. B. & Rahbek, A. (2020), 'Bootstrapping noncausal autoregressions: With applications to explosive bubble modeling', *Journal of Business & Economic Statistics* **38**(1), 55–67.

Chen, T. & Guestrin, C. (2016), XGBoost: A scalable tree boosting system, in 'Proceedings of the 22nd ACM SIGKDD International Conference on Knowledge Discovery and Data Mining', pp. 785–794.

Dalmasso, N., Pospisil, T., Lee, A. B., Izbicki, R., Freeman, P. E. & Malz, A. I. (2020), 'Conditional density estimation tools in python and R with applications to photometric redshifts and likelihood-free cosmological inference', *Astronomy and Computing* **30**, 100362.

Davis, R. A. & Song, L. (2020), 'Noncausal vector AR processes with application to economic time series', *Journal of Econometrics* **216**(1), 246–267.

de Truchis, G., Fries, S. & Thomas, A. (2025), 'Forecasting extreme trajectories using seminorm representations'. Working paper.

de Truchis, G. & Thomas, A. (2025), Laurent series expansion for  $MA(\infty)$  representation of mixed causal-noncausal autoregressive processes, LEDa Working Paper WP 2025-06, LEDa, Université Paris Dauphine, PSL.

Dey, B., Newman, J. A., Andrews, B. H., Izbicki, R., Lee, A. B., Zhao, D., Rau, M. M. & Malz, A. I. (2022), 'Re-calibrating photometric redshift probability distributions using feature-space regression'. arXiv:2110.15209.

Dey, B., Zhao, D., Andrews, B. H., Newman, J. A., Izbicki, R. & Lee, A. B. (2025), 'Towards instance-wise calibration: Local amortized diagnostics and reshaping of conditional densities (LADaR)'.

Diebold, F. X. (2017), 'Forecasting in economics, business, finance and beyond'.

Fries, S. (2022), 'Conditional moments of noncausal alpha-stable processes and the prediction of bubble crash odds', *Journal of Business & Economic Statistics* **40**(4), 1596–1616.

Fries, S. & Zakoian, J.-M. (2019), 'Mixed causal-noncausal AR processes and the modelling of explosive bubbles', *Econometric Theory* **35**(6), 1234–1270.

Giancaterini, F., Hecq, A., Jasiak, J. & Manafi Neyazi, A. (2025), 'Bubble detection with application to green bubbles: A noncausal approach'.

Gourieroux, C. & Jasiak, J. (2016), 'Filtering, prediction and simulation methods for noncausal processes', *Journal of Time Series Analysis* **37**(3), 405–430.

Gourieroux, C. & Jasiak, J. (2018), 'Misspecification of noncausal order in autoregressive processes', *Journal of Econometrics* **205**(1), 226–248.

Gourieroux, C. & Jasiak, J. (2023), ‘Generalized covariance estimator’, Journal of Business & Economic Statistics **41**(4), 1315–1327.

Gourieroux, C. & Jasiak, J. (2025), ‘Nonlinear fore(back)casting and innovation filtering for causal-noncausal VAR models’. Last updated July 2025.

Gourieroux, C., Jasiak, J. & Monfort, A. (2020), ‘Stationary bubble equilibria in rational expectation models’, Journal of Econometrics **218**(2), 714–735.

Gourieroux, C., Lu, Y. & Robert, C.-Y. (2025), ‘The causal-noncausal tail processes’.

**URL:** <https://arxiv.org/abs/2506.04046>

Gourieroux, C. & Zakoian, J.-M. (2017), ‘Local explosion modelling by non-causal process’, Journal of the Royal Statistical Society Series B **79**(3), 737–756.

Guillaumin, A. P. & Efremova, N. (2024), ‘Tukey g-and-h neural network regression for non-gaussian data’.

Guo, C., Pleiss, G., Sun, Y. & Weinberger, K. Q. (2017), On calibration of modern neural networks, in ‘Proceedings of the 34th International Conference on Machine Learning’.

Hansen, P. R., Lunde, A. & Nason, J. M. (2011), ‘The model confidence set’, Econometrica **79**(2), 453–497.

Hecq, A. & Velasquez-Gaviria, D. (2025), ‘Non-causal and non-invertible ARMA models: Identification, estimation and application in equity portfolios’, Journal of Time Series Analysis **46**(2), 325–352.

Hecq, A. & Voisin, E. (2021), ‘Forecasting bubbles with mixed causal-noncausal autoregressive models’, Econometrics and Statistics **20**, 29–45.

Izbicki, R. (2017), ‘Converting high-dimensional regression to high-dimensional conditional density estimation’, Electronic Journal of Statistics **11**(2), 2800–2831.

Jasiak, J. & Neyazi, A. M. (2025), ‘Gcov-based portmanteau test’.

**URL:** <https://arxiv.org/abs/2312.05373>

Kull, M., Perello-Nieto, M., Kängsepp, M., Silva Filho, T., Song, H. & Flach, P. (2019), Beyond temperature scaling: Obtaining well-calibrated multiclass probabilities with Dirichlet calibration, in ‘Advances in Neural Information Processing Systems’.

Lanne, M. & Luoto, J. (2016), ‘Noncausal bayesian vector autoregression’, Journal of Applied Econometrics **31**(7), 1392–1406.

Lanne, M., Luoto, J. & Saikkonen, P. (2012), ‘Optimal forecasting of noncausal autoregressive time series’, International Journal of Forecasting **28**(3), 623–631.

Lanne, M. & Saikkonen, P. (2011), ‘Noncausal autoregressions for economic time series’, Journal of Time Series Econometrics **3**(3).

Manafi Neyazi, A. (2025), ‘Generalized covariance estimator under misspecification and constraints’.

Moniz, N., Branco, P. & Torgo, L. (2017), ‘Resampling strategies for imbalanced time series forecasting’, International Journal of Data Science and Analytics **3**(3), 161–181.

Nadaraya, E. A. (1964), ‘On estimating regression’, Theory of Probability & Its Applications **9**(1), 141–142.

Nolan, J. P. (2020), Univariate Stable Distributions: Models for Heavy Tailed Data, Springer Series in Operations Research and Financial Engineering, Springer, Cham.

Nyberg, H. & Saikkonen, P. (2014), ‘Forecasting with a noncausal VAR model’, Computational Statistics & Data Analysis **76**, 536–555.

Petropoulos, F. et al. (2022), ‘Forecasting: Theory and practice’, International Journal of Forecasting **38**(3), 705–871.

Ramsay, J. O. (1988), ‘Monotone regression splines in action’, Statistical Science **3**(4), 425–441.

Ribeiro, R. P. & Moniz, N. (2020), 'Imbalanced regression and extreme value prediction', Machine Learning **109**(9-10), 1803–1835.

Rosenblatt, M. (1969), Conditional probability density and regression estimators, in P. R. Krishnaiah, ed., 'Multivariate Analysis II', Academic Press, pp. 25–31.

Rosenblatt, M. (2000), Gaussian and Non-Gaussian Linear Time Series and Random Fields, Springer.

Rothfuss, J., Ferreira, F., Boehm, S., Walther, S., Ulrich, M., Asfour, T. & Krause, A. (2020), 'Noise regularization for conditional density estimation'.

Rothfuss, J., Ferreira, F., Walther, S. & Ulrich, M. (2019), 'Conditional density estimation with neural networks: Best practices and benchmarks'.

Samorodnitsky, G. & Taqqu, M. S. (1996), 'Stable non-gaussian random processes: Stochastic models with infinite variance', Bulletin of the London Mathematical Society **28**(5), 554–555.

Saïdi, S. (2023), Noncausal Models: Unit Root Tests and Forecasting, PhD thesis, CY Cergy Paris University.

Scott, D. W. (1992), Multivariate Density Estimation: Theory, Practice, and Visualization, Wiley Series in Probability and Statistics, John Wiley & Sons.

Shi, J., Shirali, A. & Narasimhan, G. (2024), 'ReFine: Boosting time series prediction of extreme events by reweighting and fine-tuning'.

Steininger, M., Kobs, K., Davidson, P., Krause, A. & Hotho, A. (2021), 'Density-based weighting for imbalanced regression', Machine Learning **110**(9-10), 2187–2211.

Wasserman, L. (2006), All of Nonparametric Statistics, Springer Texts in Statistics, Springer.

Watson, G. S. (1964), 'Smooth regression analysis', Sankhyā: The Indian Journal of Statistics, Series A **26**(4), 359–372.